significantly, when the Einstein field equations are satisfied, we have

$$T_{\alpha\beta\gamma}{}^{\mu}{}_{;\mu}=0, \tag{4.1}$$

where the semicolon denotes covariant differentiation. When the Riemannian manifold permits Killing vector fields ξ^{μ}, we return to a situation strikingly similar to that of the linearized theory. For if we define

$$T^{\rho}=(\sqrt{g})\xi^{\alpha}\xi^{\beta}\xi^{\gamma}T_{\alpha\beta\gamma}{}^{\rho}, \tag{4.2}$$

then if follows from Eq. (4.1) that

$$T^{\rho}{}_{,\rho}=0, \tag{4.3}$$

where a comma again denotes ordinary differentiation. That is, we have again obtained a true constant of the motion which generates a proper canonical mapping closely related to that of the linearized theory.

In general there do not exist Killing fields in the solutions of the Einstein field equations. However, the fact that Eq. (4.1) remains valid gives rise to the expectation that the superenergy generates proper canonical transformation in the full nonlinear theory, closely related to the third derivative of the metric (as computed in some preferred coordinate system). Investigation of this conjecture is currently being pursued. The significance of an affirmative conclusion to this investigation for the quantization program has been indicated in the introduction to this paper. For the relationship between the space-time translations and the proper canonical transformations generated by the superenergy is conspicuous.

PHYSICAL REVIEW VOLUME 164, NUMBER 5 25 DECEMBER 1967

Search for an Electron-Proton Charge Inequality by Charge Measurements on an Isolated Macroscopic Body*†

R. W. STOVER,‡ T. I. MORAN,§ AND J. W. TRISCHKA
Syracuse University, Syracuse, New York
(Received 11 August 1967)

A new method is reported for testing the electrical neutrality of matter containing an equal number of protons and electrons. A small iron spheroid was magnetically suspended in a uniform, horizontal electric field in such a manner that it was possible to measure electric deflecting forces small enough to detect 0.03 proton charge on the spheroid. An upper limit to the charge difference between the proton and electron, defined by $f=1+$(electron charge)/(proton charge), was found to be $|f|\leq 0.8\times10^{-19}$. It was necessary to assume: (neutron charge) = (electron charge) + (proton charge). Values of f in the range $0.8\times10^{-19}<|f|<2.8\times10^{-19}$ were excluded, and the probability that $|f|>0.8\times10^{-19}$ is not greater than 0.2. A by-product of the measurements was the finding that the iron spheroids contained less than 1 quark in 2.5×10^{18} nucleons. The measurements also permitted an estimate that the absolute electric charge on 2-eV photons is less than 10^{-16} proton charge.

I. INTRODUCTION

THE equality of the magnitudes of the electric charges of the proton and electron is an empirical discovery which remains as one of the fundamental mysteries of atomic physics. The very great experimental precision of this equality rests on measurements made during the last forty years,[1–4] although most of these measurements have been made in the last decade, the best of these being those by Hillas and Cranshaw (1959),[2] whose limiting accuracy sets an upper bound on the equality of 2 parts in 10^{21}.

Stimuli, other than curiosity, to experiments to look for a charge inequality between the proton and the electron have come, at various times, from suggestions that, if present, it might explain: (1) the magnetic field of the earth,[1] (2) the expansion of the universe,[5] (3) baryon conservation.[6] Items (1) and (2) are precluded by several experiments.[1–4] Any charge inequality, however small, would be sufficient to account for baryon conservation, if charge conservation is assumed.

In order to avoid deceptions arising from the systematic errors in a particular experimental method it is important to have several different experimental

* Supported in part by grants from the National Science Foundation, and, in the beginning, by the Office of Naval Research and the Office of Scientific Research.

† Submitted by R. W. Stover in partial fulfillment of the requirements for the degree of Doctor of Philosophy at Syracuse University.

‡ Present address: Xerox Corporation, Webster, New York, NASA fellow 1964–1966.

§ Present address: University of Connecticut, Storrs, Connecticut.

[1] A. Piccard and E. Kessler, Arch. Sci. Phys. et Nat. **7**, 340 (1925).

[2] A. M. Hillas and T. E. Cranshaw, Nature **184**, 892 (1959); *ibid.*, **186**, 459 (1960).

[3] J. G. King, Phys. Rev. Letters **5**, 562 (1960).

[4] J. C. Zorn, G. E. Chamberlain, and V. W. Hughes, Phys. Rev. **129**, 2566 (1963).

[5] R. A. Lyttleton and H. Bondi, Proc. Roy. Soc. (London), **A252**, 313 (1959).

[6] G. Feinberg and M. Goldhaber, Proc. Natl. Acad. Sci. U. S. **45**, 1301 (1959).

techniques of comparable accuracy for prosecuting the search for a possible charge inequality between the proton and the electron. Three general methods have already been developed. They are: (1) the gas-efflux method, (2) the molecular-beam method, and (3) the isolated-body method. Before the performance of the experiment reported here the results from the use of these various methods were not of comparable accuracy, the gas-efflux method giving the best results and the isolated-body method the poorest.

This paper is a report of a considerable improvement in results obtained by the isolated-body method, heretofore exemplified by the Millikan oil-drop experiment,[7,8] in which any deviation of the charge on the oil-drop from an integral number of proton charges can be regarded as indicative of a failure of charge neutrality in a body containing an equal number of protons and electrons. The present results have been obtained through a new technique for isolating the body whose charge is to be measured.[9]

In our experiment an iron spheroid, about 0.1 mm in diameter, is suspended magnetically by a technique developed by Beams.[10] The spheroid is held at rest in the air space between two vertical, parallel metal electrodes whose separation is about 3 mm. When the spheroid is charged a horizontal force on it is created by an electric field set up in the region between two electrodes. In order to detect this force, when the charge is a small fraction of a proton charge, it is necessary to shape the magnetic field in such a way that the horizontal magnetic force restoring the spheroid to an equilibrium position is very small. Any deviation of the spheroid from its equilibrium position is detected by the motion of its shadow on a photocell. After deflection by an electric field, the spheroid is restored to its undeflected position by means of the horizontal force from a second magnetic field, other than the suspension field, whose effect is proportional to the current in the windings of the second magnet. Thus, our method is a null method in which the charge of the spheroid is proportional to the current in the windings of an air-core coil.

There is an important, heretofore unrecognized, set of restrictions on the interpretation of the charge measurement made by the suspended-body method. This set of restrictions is related to the fact that if there really were a charge on "neutral" matter, i.e., matter containing an equal number of protons and electrons, a sufficient accumulation of this matter would produce a charge equal in magnitude to one proton charge; a further accumulation would result in a charge magnitude of two proton charges, etc. In a macroscopic body, integral numbers of accumulated protonic charges could be readily neutralized through its gaining or losing electrons; hence, its nominal condition of charge neutrality, as determined by macroscopic measurements, is related to the charge q on the same body, when the number of electrons and protons are equal, by the equation

$$q=(n+\delta)e, \tag{1}$$

where n may be either a negative or a non-negative integer and e is the charge on the proton. The quantity δe, where $|\delta|<0.5$, we shall call the "residual charge." As a measure of the possible proton-electron charge inequality we take the quantity

$$\begin{aligned} f&=1+(\text{electron charge})/(\text{proton charge})\\ &=1+Q_-/e. \end{aligned} \tag{2}$$

If there are N nucleons in a spheroid and if the (proton +electron) and neutron mass differences are neglected, then

$$q=Nfe=(m/m_p)fe, \tag{3}$$

where m is the mass of the spheroid and m_p is the mass of the proton, whence,

$$f=(m_p/m)(n+\delta). \tag{4}$$

Because the errors in m and the errors in δ have different effects on the possible values of f, these errors will be considered separately. Suppose that observations yield a value $\delta\pm\omega$, where ω is the error in δ; then the set of possible f values is periodic with the same error, $\pm(m_p/m)\omega$, for each value of n. The errors in the mass are of two kinds, random and systematic. The random errors are those resulting from changes which occur in the mass during the set of observations used for calculating δ. These errors may be caused by abrasion of the spheroid during the suspension process, a process to be discussed later, or accumulations or loss of surface contaminants during the time of observation. These errors are negligible in the present experiments. The systematic error comes from the measurement of the mass of the spheroid. Let this systematic error in mass be $\pm\gamma$; i.e., $m=\bar{m}\pm\gamma$. Let Eq. (4) be regarded as a linear plot of f versus n, then the effect of γ is to give a range of possible slopes and intercepts to this straight line. This idea is represented graphically in Fig. 1, where the special case $\delta=0$ and $f>0$ has been chosen for the sake of simplicity. The two straight lines marked $+\gamma$ and $-\gamma$ represent the lines for the stated error range in m. The cross-hatched areas in the right part of the figure designate the possible values of f resulting from the error in δ alone. The cross-hatched areas to the left designate the possible values of f resulting from both errors. Because the periodicity of f values depends on the slope of the line it is clear that above a certain f value the error intervals on the

[7] R. A. Millikan, *Electrons (+ and −), Protons, Photons, Neutrons and Cosmic Rays* (University of Chicago Press, Chicago, 1935).

[8] V. D. Hopper and T. H. Laby, Proc. Roy. Soc. (London), **178A**, 243 (1941).

[9] The isolated body method reported here was first proposed by two of us. Cf. J. W. Trischka and T. I. Moran, Bull. Am. Phys. Soc. **5**, 241 (1959).

[10] J. W. Beams, C. W. Hulburt, W. E. Lotz, Jr., and R. M. Montague, Jr., Rev. Sci. Instr. **26**, 1181 (1955).

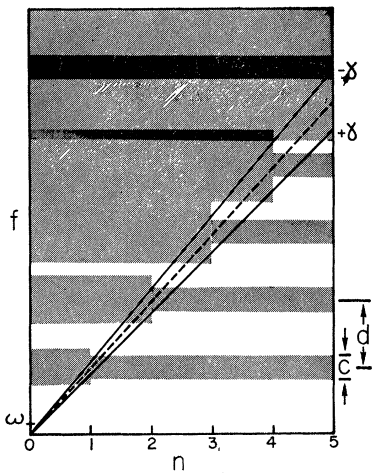

FIG. 1. Chart of possible and excluded values of f, determined from measurements on a single spheriod.

set of lines between $+\gamma$ and $-\gamma$ in Fig. 1 will overlap and there will be a continuum of possible values of f.

The above analysis suggests that a proper summary of results of an experiment with a single spheroid requires three separate statements. Let us again use $\delta=0$ as an example. First, the possibility that $-\omega<f<+\omega$ cannot be excluded by the experiment. Second, the open regions, those not cross-hatched, on the left side of Fig. 1 are regions of excluded values of f.

The third statement requires further discussion. Although the cross-hatched regions, on the left in Fig. 1, represent regions of possible values of f, the probability that f lies in these regions can be stated. In an experiment with a single spheroid the regions of possible f are of the same kind as those shown on the right in Fig. 1. Although the accurate numerical values of either the excluded or possible values of f are subject to doubt because of the systematic error in the determination of m, nevertheless, the probability that f lies in the region above $f=\omega$ is clearly the ratio of the values designated by the cross-hatching to the total set of values; viz., c/d. Therefore, the third statement is as follows: The probability that f has a value $f>\omega$ is not greater than c/d. It is easily seen that measurements made on additional spheroids of properly chosen masses can increase the excluded region of possible f values between $f=\omega$ and some higher point above which all values of f are possible. Complete measurements were made with only one spheroid in the present experiments.

It is a common feature of all present methods that they are fundamentally based on the idea of testing the charge neutrality of whole atoms. With the exception of H^1 the atoms contain neutrons. Therefore the neutrality of the neutron must be an additional subject of observation. In order to measure separately the charge equality of the proton and electron and the charge neutrality of the neutron, it is necessary to use at least two different materials in which the neutron-proton ratio is different. When this has not been done, as is the case for several experiments, including the present one, it has been assumed that the possible charge on the neutron was the same as the possible electron-proton charge sum. That this is not necessarily so can be seen from the application of charge conservation to the neutron decay process. Whence, the charge difference between the neutron n and the antineutrino $\bar{\nu}$ is

$$Q_n-Q_{\bar{\nu}}=fe=e+Q_-. \tag{5}$$

The assumption that the neutron charge is equal to the sum of the proton and electron charges requires that the charge of the antineutrino be zero.

TABLE I. Upper limits of $|f|$ and $|Q_n|$ as determined by various experiments.

	Method[g]	Upper limit of $\|f\|$	Upper limit of $\|Q_n\|$	Upper limit of $\|f\|$ (assuming $Q_n=fe$)
Millikan[a]	SB			10^{-16}
Piccard and Kessler (1925)[b]	GE			5×10^{-21}
Hopper and Laby (1941)[c]	SB			5×10^{-17}
Hillas and Cranshaw (1959)[d]	GE	4×10^{-20}	$4\times10^{-20}\,e$	2×10^{-21}
King (1960)[e]	GE	2×10^{-20}	$1\times10^{-19}\,e$	7×10^{-21}
Zorn, Chamberlain, Hughes (1963)[f]	MB	36×10^{-18}	$26\times10^{-18}\,e$	5×10^{-19}
Present work	SB			1×10^{-19}
Present work (potential sensitivity)	SB			2×10^{-20}

[a] Reference 5.
[b] Reference 1.
[c] Reference 8. The estimate of $|f|$ was made by the present authors.
[d] Reference 2.
[e] Reference 3. Values listed for King are intended only to indicate the potential sensitivity of his apparatus. Private communication indicates there are some inconsistencies in his results.
[f] Reference 4.
[g] SB: suspended body; GE: gas efflux; MB: molecular beam.

Table I shows the results from previous experiments and the lower limits reached in the present experiment, for which the complete results are presented in a necessarily more complicated form in the last section of this paper.

II. GENERAL DESCRIPTION OF THE EXPERIMENT

Because the apparatus consists of two nearly independent systems, this section will be divided into two parts: (1) the suspension system and (2) the measuring system.

A. Suspension System

Figure 2 shows a schematic diagram of the apparatus, and Fig. 3 gives a somewhat simplified side view of the physical arrangement. Figure 3 is approximately to scale. The distance between the lamp L and the sus-

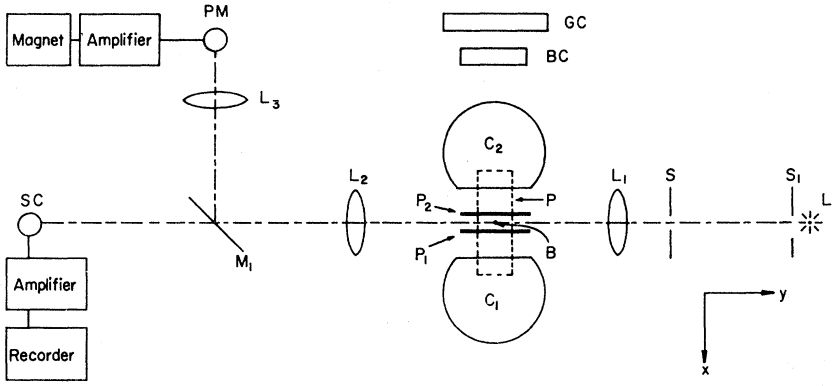

FIG. 2. Schematic diagram of suspension and measuring systems.

pended spheroid B is 65 cm. The iron spheroid is held in suspension, in air at atmospheric pressure, between the electrodes P_2 and P_1 by an electromagnet whose field is vertical, the z direction in Figs. 2 and 3, at the stable position of the spheroid. The pole face of the magnet is shown in Fig. 2 by the dashed rectangle with B at its center. The vertical distance from the pole face (Fig. 3) to B is about 2 cm.

Because of the inherent mechanical instability of the spheroid in the magnetic field, a servo system is used for maintaining the magnet current precisely at the value required to keep B at a fixed height. Except for minor changes our system is a copy of that used by Beams et al.[10] The W projection lamp L illuminates the slit S_1 whose image is focused by the lens L_1 on B. The combined shadows of the spheroid and S_1 are focused on the photomultiplier tube PM by means of the lenses L_2 and L_3. M_1 is a beam splitter. A stable operating condition is achieved when B is partially in the shadow of the lower edge of the slit. In this condition any vertical motion of B causes a change in the photocurrent at PM. Such a change, after amplification with the proper phase, produces a change in the magnet current in the direction appropriate for restoration of B to its stable position.

The horizontal stability of the spheroid is assured by the shape of the pole face of the magnet, shown in detail in Fig. 4(a) and (b), and the coils C_1 and C_2, shown in Fig. 4(c) and (d). Reference axes for Fig. 3(d) are the same as those for Fig. 3(a). C_1 and C_2 will hereafter be called "bottle coils" for reasons which will become apparent below.

The magnetic dipole forces on the spheroid are given by

$$\mathbf{F}=(\boldsymbol{\mu}\cdot\nabla)\mathbf{B}, \tag{6}$$

where the induced magnetic dipole moment $\boldsymbol{\mu}$ is assumed proportional to $\mathbf{B}$. The z component of the dipole being dominant, we ignore the other components in the explicit expression for the force, and write

$$F_x=\mu_z(\partial B_z/\partial x)\equiv\mu_z B_{zx},\quad F_y=\mu_z B_{zy},\quad F_z=\mu_z B_{zz}. \tag{7}$$

Hereafter the notation for all fields, magnetic or electric, will be one in which the first subscript symbolizes the direction of a field component and subsequent subscripts stand for differentiation. F_x in Eq. (7) illustrates the explanation of this notation.

The adjustment of F_z by the means of the servosystem has already been discussed. The highly divergent shape of the magnetic field in the yz plane, for $B_z>0$, results in a large negative value of B_{zyy}, and hence a strong restoring force along the axis of the light beam. The long x dimension of the pole face makes B_{zxx} very

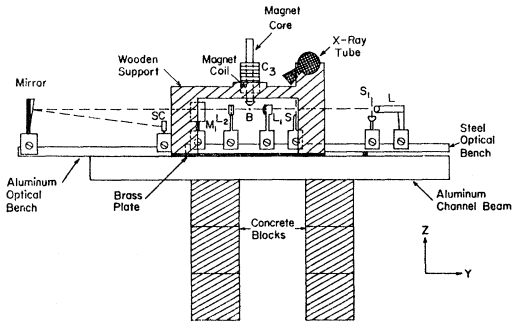

FIG. 3. Profile of apparatus. Dashed line is the path of the light beam.

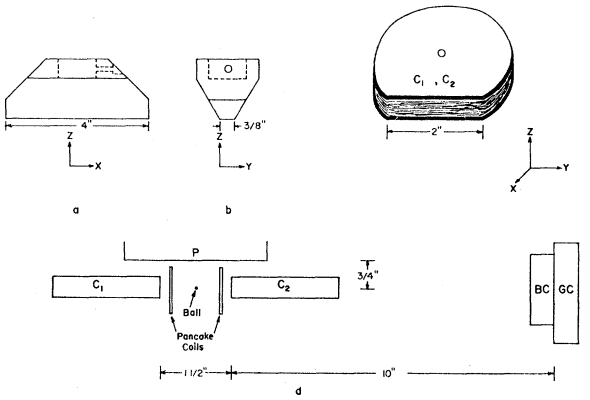

FIG. 4. (a and b) Pole piece, (c) bottle coils, (d) view in y direction of coils controlling magnetic field.

small. The bottle coils give sufficient control of this field derivative to make it positive (nonequilibrium condition), zero, or negative (equilibrium condition). The smallest practical restoring force in the x direction resulted in a period of oscillation of 9 sec. For an optimum ratio of signal to noise, however, shorter periods, of the order of 4.5 sec, were used in our measurements.

A typical spheroid had a diameter of 10^{-2} cm. When magnetically suspended, its stability was such that observations with a 50-power microscope showed no "hunting" in any direction greater than 2μ, the least count of the observation. When observed with the measuring system the suspended spheroid showed random changes in its x position of about 1μ, during a time interval of 10 sec, the standard interval of an observation.

B. Measuring System

1. General Principles

The key to understanding the measuring system lies in the forces exerted on the spheroid when voltage is applied to the electrodes P_1 and P_2, Fig. 2. Magnetostatic and electrostatic forces were found sufficient to explain all observed motions of the spheroid, both with and without the electric field between P_1 and P_2. When the electric field is applied, two, and only two, general types of forces should be evident, those proportional to the field E_x and those proportional to E_x^2. The presence of only these two types of forces was carefully validated by experiments conducted at several different values of E_x.

Since we seek a force proportional to E_x, an electric monopole force, it is necessary to eliminate effects from the forces proportional to E_x^2. Because the dominant force of this type is caused by the interaction of the induced electric dipole moment in the conducting spheroid and the field gradient E_{xx}, these forces have been called "gradient forces". Their effect on the experiment was distinguished from effects proportional to E_x through observations made with the field in each of its two possible directions, the gradient forces being unaffected by the reversal of the sign of the field and the forces proportional to E_x changing sign with the change in sign of E_x.

If the only force proportional to E_x had been the monopole force, the performance of the experiment would have been relatively easy. Unfortunately, there is a host of other important forces proportional to E_x. We have called these "pseudocharge" forces. Predominant among these are those caused by the presence of fixed electric dipole moments on the surface of the spheroid and on the surfaces of the electrodes. We were able to find and classify thirteen different pseudocharge forces. All of these were either measured directly or eliminated. These forces are discussed in detail in Sec. III.

The calibration of the forces produced by the electric field is readily achieved because the apparatus is capable of detecting forces caused by changes much less than that caused by one proton. The apparent charge q' on the spheroid, as measured by our apparatus, is given by

$$q'=(n'+\delta')e\,, \tag{8}$$

where n' is an integer and $\delta'e$ is the apparent residual charge, to be distinguished from the residual charge δe, because of the presence of pseudocharge forces. In Eq. (8) the integer n' is controlled by adding or subtracting charges from the spheroid by the use of x rays. When the change in force caused by changing n' by one unit is noted, the force corresponding to one proton charge is thereby measured and all forces can be calibrated in units of this standard force, or found absolutely from E_xe.

2. Components

Lens L_2, Fig. 2, focuses an image of the spheroid B on a silicon solar cell SC where a rectangular mask is placed so that only a narrow, horizontal strip of the image affects the cell. With this arrangement only horizontal motions of B produce changes in the photocurrent, and small vertical motions have no effect. The amplified output of the photocell drives a pen recorder.

Null measurements require the cancellation of both types of electrostatic forces. The gradient forces are balanced by an automatic electronic system attached to the electrodes P_1 and P_2. A voltage proportional to the electrode voltage is squared and fed to a current amplifier whose output provides current to a flat coil GC, Fig. 2. The magnetic field gradient from GC interacts with the magnetic moment of B to produce a force exactly cancelling the electrostatic gradient force. The forces proportional to the field are balanced by means of the coil BC, whose driving current is adjusted manually and read on a precision ammeter. The value of the current in BC when the pen recorder indicates no deflection of the spheroid, upon reversal of E_x, is directly proportional to the force E_xq'.

The field E_x is reversed in 10-sec intervals by means of an automatic timing and switching system whose output electronically controls the balance of a bridge circuit intervening between a fixed-voltage dc power supply and the field electrodes x rays, Fig. 3, are used to control the charge on the spheroid, through the ionization of the air surrounding it, a technique explained in detail by Millikan.[7] The x-ray beam is used both to discharge the spheroid immediately after suspension, when it is highly charged, and to control the charge during experiments.

C. Important Details of the Apparatus

The iron spheroids were made from commercial grade iron powder by a melting and refreezing technique

TABLE II. Physical parameters of the spheroids.

Parameter[a]	No. 1	No. 2	No. 3
Mass (kg)	4.1×10^{-9}	4.6×10^{-9}	4.3×10^{-9}
ξ (m)	5.00×10^{-5}	5.19×10^{-5}	5.07×10^{-5}
η (m)	4.93×10^{-5}	5.16×10^{-5}	5.00×10^{-5}
ζ (m)	5.08×10^{-5}	5.22×10^{-5}	5.16×10^{-5}
p_i (m C)	7.0×10^{-18}	7.8×10^{-18}	7.4×10^{-18}
ϵ^2	0.03	0.01	0.03

[a] p_i is the value of the induced dipole with an applied field of $E = 5 \times 10^5$ V/m. $\epsilon = [1 - (\eta/\xi)^2]^{1/2}$.

described elsewhere.[11] When not in use the spheroids, held on the tips of sewing needles, were stored in oil. Before use they were cleaned with Radiacwash and acetone. The three spheroids used in our experiments were spherical to better than 2%. However, deviations from sphericity were important in the analysis of the torques acting on the suspended spheroids, and measurements were made with a 300-power microscope to determine the principal axes of the ellipsoid best fitting the shape of our spheroids. Table II shows the results of these measurements, where ξ, η, and ζ are the lengths of the semiaxes. The mass given in Table II was obtained from the measured volume and the assumption that the density was that for pure iron, 7.9 g/cm^3.[12] The estimated error in mass measurements was 15%.

Skelly has constructed a fishpole balance in this laboratory for the purpose of measuring the relative masses of spheroids to about 1 percent.[13] The balance is quite important if the excluded region of possible f values is to be increased through the use of several spheroids, as mentioned in the introduction. For reasons given later, the balance was not used in our measurements.

Permanent magnetism in the spheroids was removed through ac demagnetization before their insertion in the apparatus. However, they soon acquired a small amount of permanent magnetism as demonstrated by the fact that the direction of the magnetic suspending field determined which of the two hemispheres of the suspended spheroid was uppermost.

The electrodes P_1 and P_2 were incorporated in a closed, brass box as shown in Fig. 5. The x direction in the apparatus was the vertical direction, in the side view of Fig. 5, when measurements were being made. However, in order to suspend the spheroid it was necessary to rotate the electrode box so that the plane of P_1 was horizontal, the spheroid resting on P_1. To this end the box was supported in such a way that it could be rotated through 90 degrees about the y axis. The box mount was in turn supported by an engine capable of being set on measured positions in the x, y, and z directions to within 0.0002 in. Rotation about the z axis was also possible.

In order to make P_1 and P_2 parallel, the orientation of P_2 was adjusted by means of three Nylon screws $S_{1,2,3}$. P_1 was at the same potential as the other walls of the box and P_2 was insulated with Lucite. The high-voltage lead L_4 passed through the center of the insulator. The light beam entered and left the box through two glass windows W_1 and W_2 made from microscope cover glasses. These were remote from the observation region because it was found in earlier experiments with glass boxes that charges on the glass seriously affected the experimental results. No difficulties of this kind were encountered with the box in Fig. 5. As a precaution the windows were coated with a commercial antistatic liquid, SNAP. The x-ray window was also of glass, and remote enough from the measuring region to cause no problems. This window was also used for visual observations of the spheroid with a 50-power microscope. Small metal tubes T_1 and T_2 permitted the changing of the gas within the box, which was always operated at atmospheric pressure. The interior of the box was gold-plated, and electrodes were either gold-plated, or, at the end of our experiments, made of gold.

P_1 and P_2 were about 2 cm in diam with a gap between them of about 0.3 cm. In order to examine the character of the pseudocharge forces it was important to examine the forces on the spheroid over as large a region of the gap as possible. The region in which significant measurements could be made was called the "accessible region." It was delimited by

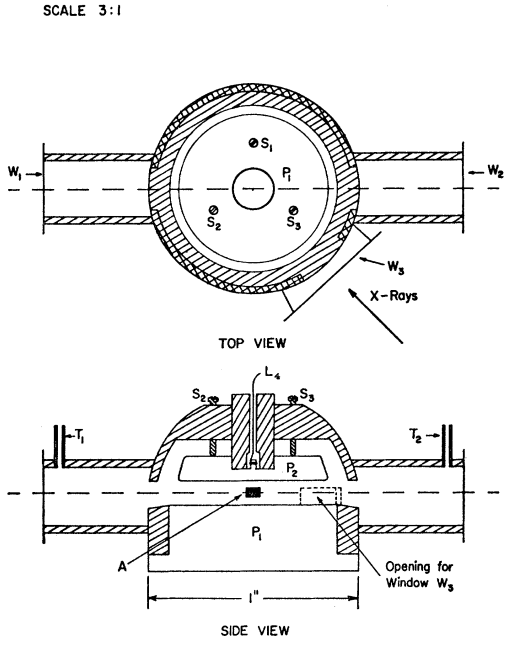

FIG. 5. Cross sections of electrode box.

[11] R. W. Stover and J. W. Trischka, Rev. Sci. Instr. 33, 694 (1962).

[12] *American Institute of Physics Handbook*, (McGraw-Hill Book Company, New York, 1963), 2nd edition.

[13] J. Skelly, Rev. Sci. Instr. 38, 985 (1967).

fringe effects, images of the induced dipole and obstruction of the light beam by the box. This region was in the shape of a disk, centered in the gap, 1 mm wide in the x direction and 4 mm in diam (cf. region A in Fig. 4.)

The electrode box was so mounted that it was readily rotatable through 90°, about the axis of the light beam. The position in which the electrodes were horizontal was required for the purpose of suspending the spheroid in the light beam. Before suspension the spheroid lay on P_1, Fig. 5, at its center. The spheroid was accelerated upward into the light beam by means of blows struck on the bottom of the box-support by a brass rod. The rod was motor driven by means of a rotating cam. The proper positioning of the box, the setting of the appropriate magnetic suspending field, and the adjustment of the strength of the blows struck by the brass rod were an art, although once success was achieved it was readily achieved again in subsequent runs with the same spheroid. After the spheroid was suspended, the electrode box was rotated to the position in which the electrodes were vertical.

Some of the coils used for maintaining and controlling the magnetic field remain to be mentioned. The coils C_3 in Fig. 3, in series with the bottle coils, were needed to cancel the contribution to B_z made by the latter coils. The pancake coils, Fig. 4(d), were spiral wound coils, 1.5 mm thick, for altering the magnetic field configuration in testing for those pseudocharge forces which involved the magnetic field. These coils were designed to reduce B_{xx} to zero. Another set of coils, not shown, were Helmholtz coils with axes in the y direction, their purpose being to produce a constant value of B_y. A third pair of coils, important for examining pseudocharge effects, were wound on a parabolic form, had axes in the x direction, and were used to change B_{xy} independently of B_{xx}.

Magnetic fields were measured with Hall probes, the smallest of which had an active area of 0.5 mm×1.0 mm. Table III shows the fields and gradients produced by the suspension magnet and the various field-controlling coils. The first three columns give fields used under operating conditions. The last two columns show typical fields for those coils, whose use was found unnecessary during measurements, although quite necessary for studying the nature of the pseudocharge forces.

TABLE III. Contributions to the magnetic field due to the magnet and the various coils.

Magnetic field term (emu)	Magnet	Bottle coils	Pancake coils	Parabolic coils	Helmholtz coils
B_x	<1	+3.3	+3.4	+1.6	−0.06
B_y	1	0	1.0	−39	−4.2
B_z	−320	15	0	0	0
B_{xx}	−13.8	+3.6	+10.3	0	+0.3
B_{yy}	−88.5	−0.8	−4.3	+6.7	−0.20
B_{zz}	+100	0	0	0	0
B_{yz}		−0.4	+0.6	−3	−0.5
B_{yx}	0.8	−0.5	−0.4	+0.6	−0.05

III. PSEUDOCHARGE FORCES

A. General Features

It is crucial to the proper performance of this experiment that all observed forces and torques exerted on the spheroid be explained, and that all forces and torques predicted by our model be quantitatively accounted for. In this section we will be concerned with those forces which are proportional to E, exclusive of the monopole force whose measurement is the object of our experiment.

The theoretical model, adequate to account for all observed forces and torques, was as follows.

(1) All forces and torques are a result of electrostatic and magnetostatic fields plus a constant gravitational force.

(2) The spheroid can be regarded as an ellipsoid of conductive and highly paramagnetic material with some residual permanent magnetism.

(3) The electric potentials of the surfaces of the ellipsoid, and of the surrounding conductors, are nonuniform, thus causing the ellipsoid to exhibit a permanent electric moment, and giving rise to a fixed inhomogeneous electric field between the electrodes. These are in addition to the induced dipole moment on the ellipsoid, and to the field between the electrodes P_1 and P_2, maintained by the power supply. These effects are ascribed to nonuniform surface dipole layers, but this explanation is not crucial to the experiment.

A further explanation of some features of this model may be useful. Being iron, the spheroid is ferromagnetic. However, once suspended in the magnetic field it is subjected to such small changes in this field that no hysteresis effects are observable, and its interaction with the field is very nearly linear. Hence it can be treated as being paramagnetic with some residual magnetism which is quite small because of the weakness of the magnetic fields involved, about 300 G. The evidence for some small permanent magnetism has already been given. The existence of permanent electric fields produced both by the spheroid and by the electrodes has been amply demonstrated in our studies, and, although their origin cannot be known in atomic detail, they are attributed to nonuniform dipole layers on quite general grounds. The spheroid and electrodes, being electrical conductors, will not exhibit nonuniform surface potentials caused by volume charges. Any bound, surface charges, however, whatever their origin, will attract equal and opposite image charges, thereby producing surface dipoles. Order of magnitude calculations of the fields expected from reasonable distributions of "patches," differing in work function by a

few tenths of a volt, give values in agreement with fields which would account for the observed effects. No evidence was found for electric multipoles higher than the dipole.

The various possible pseudocharge forces are listed in Table IV. Except for the first two, their individual contributions to the error in the apparent residual charge has been limited to less than $0.01e$. They can be conveniently into four types. Type I pseudocharge forces have a purely electrostatic origin. Type II originate in the rotation of the spheroid. The only rotation observed was about the z, or vertical, axis, but theoretically, unobserved rotations about the other axes could cause measurable forces under certain magnetic field conditions. Type III are forces in the x direction resulting, indirectly, from displacements in the y and z directions which are proportional to E. Type IV pseudocharge forces include all the various instrumental effects which might be mistaken for the monopole force. Let us now discuss some of these pseudocharge forces in greater detail.

B. Type I: Electric Forces

We should say a word about the notation to be used in what follows. The electric field produced by the power supply will be called the "applied field" E. The permanent field produced by the fixed dipole layers on the electrodes will be called the "fixed field" E^f. The dipole moment induced in the conducting spheroid by the applied field will be called the "induced dipole" p^i, and the permanent electric dipole moment of the spheroid will be designated by p. The dipole induced by the fixed field was negligible.

The first pseudocharge force listed in Table IV is the result of the interaction of the permanent electric dipole moment of the spheroid with the gradient of the applied electric field, and is given by the relation

$$F_x{}^f = p_x E_{xx} + p_y E_{xy} + p_z E_{xz}. \quad (9)$$

TABLE IV. List of pseudocharge forces.

Type I
1. Interaction of fixed dipole layers on the ball with applied-field derivatives.
2. Interaction of induced dipole on the ball with fixed-field derivatives.
3. Effects due to images of fixed dipole and induced dipole.
Type II
4. Induced dipole function of ball rotation.
5. Effect of rotation on ball silhouette.
6. Effect of rotation about z axis on magnetic force.
7. Effect of rotation about y axis on magnetic force.
8. Effect of rotation about x axis on magnetic force.
9. Effect of change of vertical component of magnetic dipole.
Type III
10. Effect of pseudocharge force in z direction.
11. Effect of pseudocharge force in y direction.
Type IV
12. Effect of unbalanced voltage squarer.
13. Other instrumentation effects.

To determine this force we must measure six quantities. Measurements of the rotation caused by the applied electric field yielded either a value or an upper limit for each of the three components of the fixed dipole moment. The torque about the z axis, caused by the permanent electric dipole, is given by $T_z = -p_y E_x$. E_x was calculated from a knowledge of the applied voltage and the spacing of the electrodes. T_z could be obtained from the observed rotation and a knowledge of the shape of the spheroid; hence, a value for p_y was obtainable. An upper limit on p_x was obtained from a somewhat more complicated analysis of the rotation about the z axis. An upper limit on p_z was set from the relation $T_y = p_z E_x$. Although no rotation of the spheroid about the y axis was ever visually observed, a more sensitive indicator of this rotation was afforded by a pseudocharge force resulting from a rotation, about the y axis, too small to be observed through the microscope. This pseudocharge force, No. 7 in Table IV, could be measured and controlled by use of the pancake coils.

The value for the electric field gradient E_{xx} comes from a measurement of the electric gradient force, $F = p^i E_{xx}$. Figure 6 shows E_{xx} at the mid-gap position as a function of y when $E_x = 5 \times 10^5$ V/m. Calculated values for the induced dipole p^i for each spheroid, are listed in Table II, for an applied field of $5(10)^5$ V/m. The gradient E_{xz} was found by rotating the electrodes about the y axis into the horizontal plane, and measuring $F_x = p^i E_{xz}$, p^i then being in the z direction. This measurement was followed by a rotation of the electrodes about the z axis[14] and a remeasurement of F_x. In the remeasurement E_{xy} contributed to the force.

Because E_{xz} and E_{xy} were determined largely by the degree of parallelism of the electrodes, the screws S_{1-3} were adjusted to bring the appropriate terms of Eq. (9) below the maximum acceptable values. E_{xx} was kept below the maximum acceptable value by keeping the spheroid within the accessible region. As a consequence of the above procedures pseudocharge force No. 1 was limited to a value equivalent to the monopole force on a charge of $0.01e$.

The second type I pseudocharge force listed in Table IV was caused by the interaction of the induced electric dipole moment of the spheroid with the electric field gradient set up by the fixed dipole layers on the electrodes. Because the induced dipole was in the x direction, only the x component of the electric field gradient was important, and we could express this force as $F_x{}^f = p^i E_{xx}{}^f$. A careful measurement of this force was unavoidable in order to get meaningful results. Unfortunately, the experimental uncertainties in this measurement were such as to make the final errors in the results much greater than those involved

[14] Only a few degrees of rotation was possible, but this was sufficient.

in the measurement of the apparent residual charge, $\delta' e$. To measure $E_{xx}{}^f$, the electrodes were shorted and the force $F_x{}^f = QE_x{}^f$ on a highly charged spheroid was measured at various positions along a line parallel to the x axis. The average fixed-field gradient was found from the expression $\langle E_{xx}{}^f \rangle_{\text{av}} = Q\langle \partial F_y{}^f/\partial x \rangle_{\text{av}}$. The large charge on the spheroid was obtained by an x-ray ionization method. The effects of image forces from the electrodes were important in these measurements, but these effects could be calculated with adequate accuracy and were, in addition, used in the determination of the distance between the two electrodes.

Further discussion of procedures for and the results from the measurement of this important pseudocharge force will be left to the next section.

The third type I pseudocharge force, No. 3 in Table IV, was caused by the images in the electrodes of the fixed and induced electric dipole moments of the spheroid. Calculations showed this force to be negligible.

C. Type II: Rotation Effects

Type II pseudocharge forces were caused by the rotation of the spheroid when the electric field was reversed, and were primarily due to the nonspherical shape of the spheroids. One result of a nonspherical shape was that their induced polarization was a function of their orientation in the electric field. No. 4 in Table IV is the pseudocharge force caused by the change in the interaction of the applied field gradient with the induced dipole moment. Calculations based on a knowledge of the shape of the spheroids showed this force to be negligible.

The irregular shape of the spheroid might have caused, when it was rotated by the electric field, a change in its shadow on the solar cell detector (*SC* in Figs. 1 and 2). Direct measurements to detect this effect were possible because it was not truly proportional to E but to the angle of rotation when the electric field was reversed. The stated results include the correction term for this effect, listed as No. 5 in Table IV.

Rotations of the spheroid resulted in changes in its interaction with the magnetic field, thus indirectly causing forces approximately proportional to the electric field. They are listed as pseudocharge forces Nos. 6–8 in Table IV. These forces were eliminated by proper shaping of the magnetic field. Specially designed coils, such as the pancake coils already mentioned, were installed for this purpose.

D. Other Effects

The remaining pseudocharge forces will not be discussed in detail. Table V summarizes the treatment of these forces. A check in the column headed "Calc" signifies that calculations show the effect to be insignificant. A check in the column headed "Exp" indicates that some experiment or experiments were performed that either proved the effect was insignificant or produced a correction term. A check in the column labeled "Correction" indicated corrections to the apparent residual charge were necessary. The column labeled "Maximum error" gives the approximate upper limit to the systematic error from these effects.

TABLE V. Summary of the treatment of pseudocharge forces.

Pseudocharge force[a]	Calc.	Exp.	Correction	Maximum error	Remarks
1.	X	X	X(≤0.02)	0.01	Higher-order terms possible.
2.		X		?	No estimate on error for balls No. 1 and No. 2
3.	X			0.000	
4.	X	X	X	0.005	
5.		X	X		Error included in error in δe
6.	X	X	X		
7.		X	X	0.000	
8.	X	X		0.000	
9.	X			0.005	
10.		X		0.001	
11.		X		0.000	
12.	X	X	Squarer Adj.	0.01	
13.		X		0.01	

[a] See Table IV for description of each pseudocharge effect.

Some of the entries require special comment. No. 1 has a check under Calc because of the previously mentioned calculation implying the unimportance of higher-order poles than the dipole; however, dipoles were not unimportant and corrections must be made for them. Nos. 4 and 6 have an X under "Correction" because they are automatically corrected for by the procedure that corrects for No. 5, even though we believe them to be negligible. Finally, the voltage squarer had to be carefully adjusted to ensure that pseudocharge force No. 12 was negligible.

IV. DATA AND RESULTS

Immediately after it was suspended a spheroid had a very large charge, sometimes of the order of $10^5 e$. After x rays were used to reduce the charge to a few proton charges, at which point it was safe to apply voltage to the electrodes, a determination was made of the bucking-coil current $I_{BC}{}^0$, required to balance the electric force on the spheroid. Measurements were made for several charge values, both positive and negative, and the results fitted by the method of least squares to the linear relation

$$I_{BC}{}^0(k) = ka + b, \tag{10}$$

where k is an integer. Hence, a and b were found, and yielded the apparent residual charge from $(b/a)e = \delta' e$. This required corrections for effects from the pseudocharge forces in order to get the residual charge δe.

The value of a for a given spheroid did not change with time during a given suspension nor from day to day. Hence, once a was determined for a given spheroid by the method outlined above, further determinations of b, for purposes of investigating pseudocharge forces, required the use of only one value of k. This feature permitted rapid determinations of b when the spheroid was moved from one x, y, z position to another.

Measurements were made on the three spheroids whose characteristics are listed in Table II. For reasons mentioned below, measurements sufficient for firm conclusions about f were made on only one spheroid, No. 3. Measurements were made on spheroid No. 1 for 13 different positions, covering a range of 3 mm along the y axis, in the accessible region of the electrode-box. The results of 47 measurements gave an apparent residual charge $\delta' e = (0.00 \pm 0.03)e$. When the effect of systematic errors of $0.03e$ are added to the above error, the error in the apparent residual charge is 0.04, corresponding to an "apparent" value of f, $f' \leq 1.7 \times 10^{-20}$. Measurements could not be completed on this spheroid because it was accidentally smashed when an unusually high voltage between the electrodes caused it to be driven into one of the electrodes.

Spheroid No. 2, because of its small eccentricity, underwent larger rotations when the electric field was reversed than did No. 1 and No. 3. This resulted in considerably larger errors. Hence, use of this spheroid was abandoned after enough measurements were made to verify that its behavior was consistent with our general model of the forces acting on the spheroids. From 34 measurements, in 9 different spatial positions, an apparent residual charge of $(0.04 \pm 0.08)e = \delta' e$ was found. This apparent residual charge corresponds to a value of $f' \leq (1.4 \pm 2.8)10^{-20}$. Here again, as was the case for spheroid No. 1, the absence of measurements of pseudocharge No. 2, Table IV, precluded conclusions about the actual residual charge and the actual limits on f.

An unexplained change in the surface characteristics of the electrodes occurred between measurements on spheroid No. 2 and measurements on spheroid No. 3. In the case of both spheroids No. 1 and No. 2 δ' was zero within experimental error throughout the accessible region between the electrodes. A typical set of measurements on spheroid No. 3 is shown in Fig. 6, where it is seen that δ' varied significantly as a function of the y position of the spheroid relative to the electrode center position. That this change was caused by a change in the character of the electrodes was verified by the removal of spheroid No. 3 and the reinsertion of spheroid No. 2. The results from new measurements with spheroid No. 2 were identical, within experimental error, to those obtained with No. 3. It is worth remarking at this point that the identity of these two sets of measurements furnished strong additional evidence that the observed values of δ' were not caused by pseudocharge force No. 1.

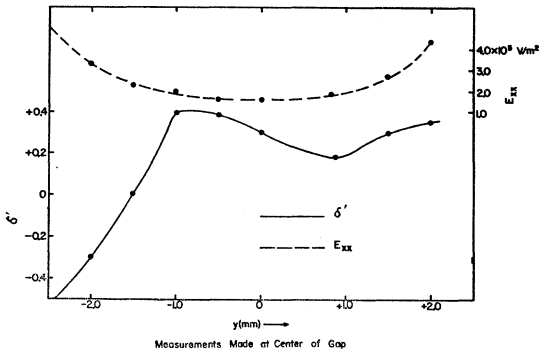

FIG. 6. Sample graphs of δ' and applied electric field gradient, E_{xx}, as function of spheroid position relative to electrode box. Spheroid No. 3.

Curves of the type shown in Fig. 5 were repeatable throughout a day of experimentation, so long as the spheroid was held in suspension. There were small changes in δ' over longer time intervals, amounting to 0.1 to 0.2 over a period of a week, but the general shape of the curve did not change. However, even the mildest treatment of the electrode surfaces with solvents produced drastic changes in δ' and its dependence on y. All efforts to return the electrodes to their original condition failed. These efforts included a variety of cleaning procedures, the replacement of gold-plated copper electrodes by pure gold electrodes, and the circulation of dry nitrogen through the electrode box. It should be noted that "clean" surfaces were not actually needed, but only a uniformity sufficient to make $E_{xx}{}^f$ vanish. Such a condition may have existed in the cases of spheroids No. 1 and No. 2.

The conditions under which final measurements were made on spheroid No. 3 were such that the only remaining correction for pseudocharge forces were for force No. 2. The method of measuring this force was described in the preceding section. Table VI shows the results of three runs, A, B and C, made at the same y position, where $\delta' = 0.25 \pm 0.05$. The quantity Q/e represents the number of protons used on the spheroid for measuring the pseudocharge force No. 2. The error in Q/e was 1%. The last column, δ' (pseudo), shows the equivalent value of δ' caused by the measured pseudocharge force. A comparison of the last two columns shows that the pseudocharge force accounts for δ' within experimental error. As a check on the origin of

TABLE VI. Results of measurements of $E_{xx}{}^f$ and relationship to intercepts.

Run	Q/e	Number of measurements	δ' (meas.)	δ' (pseudo)
A	+63 700	20	+0.25	$+0.21 \pm 0.08$
B	+44 900	20	+0.25	$+0.17 \pm 0.22$
C	−55 400	20	+0.25	$+0.20 \pm 0.15$
D	+66 700	6	+0.40	$+0.75 \pm 0.40$

δ', an additional run, D in Table VI, consisting of 6 measurements, was made at a different y position where $\delta'=0.40\pm0.05$. Again, the numbers in the last two columns agree within experimental error.

The measured residual charge, corrected for all pseudocharge forces, was

$$\delta=+0.05\pm0.18.$$

It is clear that the final results give no indication of a measurable value of f; i.e., the final result is null within the experimental error. Hence, to avoid a misleading assymetry in the statements of results, we shall conservatively base the three statements on $\delta=0.0\pm0.2$. Hence, the final results are as follows: (1) Values of f in the range $\pm0.8\times10^{-19}$ cannot be excluded; (2) excluded values of f lie in the ranges given by $0.8\times10^{-19}<|f|<2.8\times10^{-19}$; and (3) the probability that $|f|>0.8\times10^{-19}$ is not greater than 0.2.

As mentioned earlier it is possible to increase the region of excluded values of fe by the use of spheroids of different carefully selected masses. The large errors in measuring $E_{xx}{}^f$ led to our decision not to carry out this procedure because too little would have been gained by it. Although the effect of $E_{xx}{}^f$ can be expected to be greatly reduced with an increased electrode separation, this was not possible without a major revision of the apparatus, because the electrode box filled all the space available below the surface of the magnet pole face. In addition, new techniques for suspension of the spheroid would be needed.

In order to measure the charge on the neutron separately from the charge difference between the proton and the electron it would be necessary to use spheroids with a neutron-proton ratio substantially different from that for iron. Fortunately, there are other ferromagnetic materials, such as Gd, which satisfy this requirement. In the distant future it might be possible to "suspend" the spheroid by keeping it in free fall in an earth satellite, thereby eliminating the requirement for a ferromagnetic material.[15]

V. QUARKS AND PHOTON CHARGE

Although much more refined in its operation, our apparatus is of the same general type as those proposed, and in use, by others for searching for quarks whose charge is assumed to be some integral multiple of $\frac{1}{3}e$, the integer being indivisible by 3.[16] It is clear from the discussions earlier in this paper that the "suspended-body" method cannot exclude all possibilities of numbers of quarks above a minimum number; thus for a quark of charge $\frac{1}{3}e$ the presence of an integral number of quarks, for which the integer is divisible by 3, cannot be excluded. There are two ways in which a quark might be detected with our apparatus: (1) if it were created during the time of observation of the spheroid and trapped in the spheroid; (2) if it were created at some time in the past and remained trapped since then in the spheroid. In the former case the charge on the spheroid would undergo a readily detectable change of the appropriate multiple of $\frac{1}{3}e$. In the latter case, all of the problems caused by pseudocharge effects would have to be overcome, as has been done in our experiment.

No charge changes, other than those corresponding to integral numbers of e, were observed during 157 h of observation on two spheroids having a combined mass of 9 μg, or a total number of 5×10^{18} nucleons.

The residual charge on spheroid No. 3,

$$\delta e=(0.05\pm0.18)e,$$

excludes the possibility of its containing a quark, or combinations of quarks giving a charge of $\frac{1}{3}e$, $\frac{2}{3}e$, $\frac{4}{3}e$, etc. Hence, if the exceptions noted above are ignored, the sample contains less than 1 quark in 2.6×10^{18} nucleons. The iron in the spheroid came from a commercial grade iron powder of unknown terrestrial origin. This negative result can be compared with the negative result for meteoric iron,[17] of less than 1 quark in 10^{17} nucleons.

Because there seems to be some interest in the charge neutrality of photons,[18] we give here, for the sake of the record, an estimate of the charge on the photons from the tungsten light used in the suspension system of our apparatus. An increase in charge of more than $0.06e$, during several runs of at least 8 h duration, would have been detected. The upper limit for the absolute charge on a photon of energy 2 eV, the approximate average energy of the photons in the light beam, is crudely estimated as $10^{-16}e$. The authors of Ref. 18 found an upper limit of $10^{-15}e$ for the charge on 14.4-keV photons.

ACKNOWLEDGMENTS

The authors wish to thank Dr. M. Crandell and R. Finn, D. Nicholson, and J. Skelly for their aid in the laboratory. They also wish to thank G. Bacorn, G. Greene, J. Mathews, and G. Rabe for the construction of vital parts of the apparatus.

[15] P. Franken, University of Michigan, has proposed and undertaken a suspended body experiment in which the suspension system makes use of the diamagnetic properties of superconductors, (private communication).

[16] Cf., for example, G. Gallinaro and G. Morpurgo, Phys. Letters **23**, 609 (1966).

[17] W. A. Chupka, J. P. Schiffer, and C. M. Stevens, Phys. Rev. Letters **17**, 60 (1966).

[18] L. Grodzins, D. Engelberg, and W. Bertozzi, Bull. Am. Phys. Soc. **6**, 63 (1961).